Static and Dynamic Light Scattering by a Thermoreversible Gel from *Rhizobium leguminosarum* 8002 Exopolysaccharide

Tommasina Coviello† and Walther Burchard*

Institut für Makromolekulare Chemie, Universität Freiburg, 79104 Freiburg, Germany

Erik Geissler

Laboratoire Spectrometrie Physique, Université Joseph Fourier, Grenoble, 38402 St. Martin D'Heres, France

Dieter Maier

Fakultät für Physik, Universität Freiburg, 79104, Germany

Received November 7, 1996; Revised Manuscript Received January 24, 1997[⊗]

ABSTRACT: Thermally reversible gelation of an exocellular polysaccharide from the bacterium *Rhizobium leguminosarum phaseoli* strain 8002 was studied by static and dynamic light scattering (LS) and by small angle X-ray scattering (SAXS). The very stiff double helical polysaccharide spontaneously forms a gel when salt (0.1 M NaCl) is added to aqueous solutions of the polymer with concentrations larger than 1.5% (w/v). The combination of static LS and SAXS revealed a heterogeneous structure that could be described by three characteristic correlation lengths. Large globular particles with a radius of gyration of $R_G = 308 \pm 10$ nm appear embedded in a disordered medium with a correlation length of $\xi_1 = 120 \pm 20$ nm and a fractal dimension of $d_f = 1.6 \pm 0.2$. The matrix consists of entangled or associated chain sections with a cross-sectional radius of $r_c = 0.7 \pm 0.1$ nm. The large clusters have an apparent fractal dimension of $d_f = 3.2 \pm 0.3$. A third correlation length of 2.1 ± 0.2 nm found in the system may be assigned to the fairly long side chains which form a disordered layer around the double helix. The heterogeneous structure was confirmed by dynamic LS, which revealed a very slow translational mode of motion in addition to the common fast translational motion. The time domain between these two relaxation processes appeared to be filled with a spectrum of further relaxation times but could not unambiguously be analyzed by Laplace inversion of the time correlation function.

1. Introduction

In recent years a number of new polymer systems have been discovered that show gel setting on cooling and dissolution on heating. Most of these thermoreversibly gelling polymers are polysaccharides.[1−4] A well-known example is agar-agar which is extensively used in microbiology and, more recently, κ-carrageenan.[5] These two types of polysaccharides are chemically related and originate from red algae.

In this contribution a polymer is studied that belongs to the class of microbial polysaccharides. These are produced by *Rhizobia* bacteria which form symbiosis with *leguminosae* and by which binding of nitrogen is achieved. The gel formation induced by the ions of the soil has a biological function. It surrounds the roots of the plants (leguminosae) and brings about a contact of the bacterium with the host plant which may be considered as a first step in the symbiotic process.[6−8]

All the bacteria from *Rhizobia* can produce two classes of polysaccharides which differ in the composition of the backbone and side chain.[1,8] In the first class the four sugars of the repeating unit in the backbone are not charged whereas in the second class two of them are glucuronic acids. The polymer of this study belongs to the second group. Figure 1 shows schematically the polysaccharide from *Rhizobium leguminosarum bv. phaseoli*, strain 8002 (*Rhiz. Legum. bv. Phas.* 8002). Other polysaccharides from this class are produced by various *Rhizobia*. The polymers differ in length and composition of the side-chain but have in common the first two sugars linked to the backbone, and the terminal sugar always carries a (4 → 6) linked pyruvic group. Moreover, different *Rhizobia* bacteria can produce the same sugar repeating unit but with different content of acetyl and butyrate groups attached in an irregular manner to the polysaccharide. These small changes have a big influence on solubility and supermolecular structure. An example is the exopolysaccharide (EPS) from *Rhizobium trifolii*, strain TA-1, which

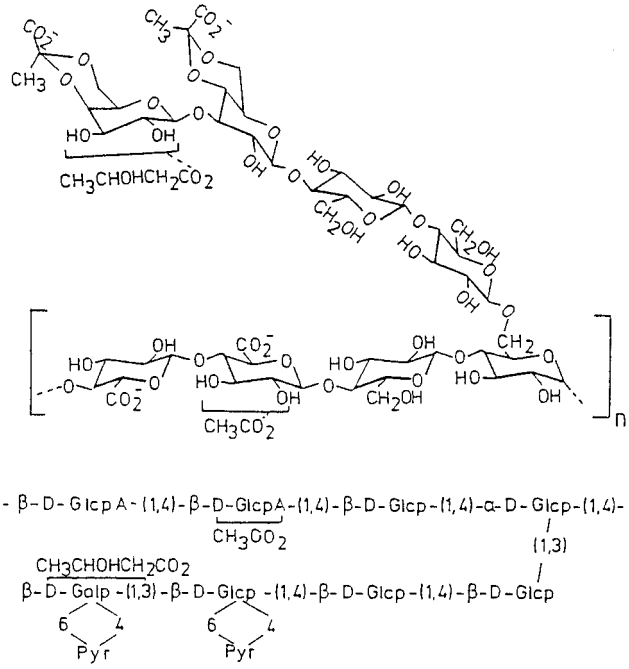

Figure 1. Repeating unit of the *R. leguminosarum ohaseoli* exocellular polysaccharide RLP 8002 EPS.

† Permanent address: Dipartimento di Studi di Chimica e Tecnologia delle Sostanze Biologicamente Attive, Università "La Sapienza", 00185 Roma, Italy.

[⊗] Abstract published in *Advance ACS Abstracts,* March 1, 1997.

S0024-9297(96)01651-8 CCC: $14.00

has the same sugar composition and sequence as the polysaccharide from *R. leguminosarum bv. phaseoli*, strain 8002 (*Rhiz. Legum. bv. Phas.* 8002). The TA-1 EPS has been studied previously,[2,8] and the dilute solution properties of the *R. leguminosarum* 8002 were reported recently.[3]

Here we now deal with the capability of these polysaccharides to form thermally reversible gels. In the present case an ionic strength of 0.1 M NaCl was sufficient to induce gelation if the polymer concentration exceeds 1% (w/v). The existence of gel formation could qualitatively be estimated by the common test tube tilting test. Such an estimation of a gel point is not accurate enough for a quantitative description of the gel or the pregel state. In fact, quantitative determination of the gel point for thermoreversible gels is a serious problem which is still much under discussion,[9−11] and for this reason it might be useful to recall how a critical point of gelation is defined for permanently cross-linked chains.

2. Critical Behavior at the Gel Point

The critical point of gelation is defined by the condition that the second moment of the molar mass or the size distribution of clusters diverges.[9] Since the weight-average of the molar mass, M_w, is directly related to this moment, the above definition is equivalent to $M_w \rightarrow \infty$ or $1/M_w \rightarrow 0$. This condition is the basis of gel point determination for systems forming permanent gels or networks. The verification of this condition can be observed by common static light scattering with the help of the equation for the scattering at zero scattering angle (forward scattering)

$$\frac{K_c}{R_{\theta=0}} = \frac{1}{M_{app}(c)} = \frac{1}{M_w} + 2A_2c + 3A_3c^2 + \dots \quad (1)$$

where $R_{\theta=0}$ is the forward scattering intensity (at scattering angle $\theta = 0$), K the usual contrast factor, and A_2, A_3, etc. the osmotic virial coefficients.

The reciprocal apparent molar mass $M_{app}(c)$ at concentration c is obtained by extrapolating the angular dependent scattering intensity to zero scattering angle, and the true molar mass of permanently cross-linked clusters is then found from eq 1 after extrapolating these data to zero concentration. This procedure, however, is not feasible with reversibly gelling systems, because on dilution dissociation of the clusters into smaller particles is induced. Hence, either a theory has to be developed which predicts A_2 and A_3 correctly as c is increased and association takes place, or a dynamic definition of the gel point has to be used. The first route was developed previously[12] and could be applied successfully to two different systems.[13,14] However, a special form of a molar mass dependence for the repulsive force, e.g. of the second virial coefficient, had to be assumed which introduced a certain ambiguity to this treatment.

A dynamic definition of the gel point can be derived from the following argument: The size of a chain or cluster in the pregel state is always connected with a certain spectrum of relaxation times and the longest of them, τ_0, is related to the hydrodynamic radius which is defined by the Stokes−Einstein relationship through the translational diffusion coefficient D_0

$$R_h = \frac{kT}{6\pi\eta_0 D_0} \quad (2)$$

The translational diffusion coefficient is given by the mean square displacement

$$\langle R^2(t)\rangle = \langle (R_0 - R_t)^2\rangle = 6D_0t \quad (3)$$

where R_t and R_0 are the positions of the particles at times t and zero, respectively. A time $t = \tau_0$ is just the time that is needed for a particle to move a distance equal to its own diameter. Consequently, since $\langle R^2(t)\rangle \sim M_w^{2\nu}$ (with $0.5 \le \nu \le 1$) also the relaxation time τ_0 must grow beyond all limits when $M_w \rightarrow \infty$.

This condition is one criterion that can be used for a determination of the reversible gel point. Another arises from the fact that clusters near the gel point have a very broad size distribution, and according to eq 2, this size distribution must have then a similar influence on the relaxation time spectrum.

Branching theories[9] (lattice percolation as well as the Flory−Stockmayer (FS) mean field theory) predict a weight fraction distribution of molar mass of the type[9]

$$w(M) = AM^{1-\tau_p} f(M/M^*) \quad (4)$$

with a characteristic, or cut-off, molar mass of

$$M^* \propto (p_c - p)^{-1/\sigma} \quad (5)$$

with the two exponents $\tau_p = 2.2$ and $\sigma = 0.4$ in lattice percolation and $\tau_p = 2.5$ and $\sigma = 0.5$ in the FS theory; p denotes the lattice site occupation and p_c the critical occupation when gelation takes place.

The type of distribution as given by eq 4 has been found now experimentally with several examples of permanent gels with a τ_p that agrees well with the lattice percolation prediction.[13−17] Unfortunately, eq 4 cannot directly be applied to reversible gels because of the repulsive forces and its influence on $M_{app}(c)$ at rather high concentrations.

However, since $R_g^2 \sim M^{2\nu}$ and if eqs 2 and 3 are considered, one should also find for the relaxation time spectrum $h(\tau)$ a power law behavior similar to eq 4, i.e.

$$h(\tau) = B\tau^{-\Delta} f(\tau/\tau^*) \quad (6)$$

where B is a normalization constant and $f(\tau/\tau^*)$ is a cut-off function for the relaxation times. This distribution of relaxation times governs both the frequency dependence of the moduli $G'(\omega)$ and $G''(\omega)$ in mechanical oscillatory rheology and the time dependence of the time correlation function $g_1(t)$ in dynamic light scattering. From the common relationship of mechanical relaxation

$$G'(\omega) = \int_0^\infty h(\tau)\frac{(\omega\tau)^2}{1+(\omega\tau)^2}\,d\tau \quad (7)$$

$$G'(\omega) = \int_{-\infty}^{+\infty} H(\tau)\frac{(\omega\tau)^2}{1+(\omega\tau)^2}\,d\ln\tau \quad (7')$$

one finds at the gel point[11]

$$G'(\omega) = \text{const} \times \omega^{\Delta} \quad (7'')$$

and, similarly, from the equivalent equation for the time correlation function

$$g_1(t) = \int_0^\infty h(\tau)\exp(-t/\tau)\,d\tau \quad (8)$$

$$g_1(t) = \text{cons} \times t^{-\Phi} \quad (8')$$

since at the gel point the cut-off function in eq 6 goes to unity. Hence, power law behavior is expected in both types of dynamic measurements when approaching the gel point. The exponent Δ and Φ are still not unambiguously defined at the present stage of theory that has been developed by Daoud and Martin.[18] Values between zero and unity appear feasible depending on the monomeric friction coefficient at high concentrations.[19]

We can summarize as follows: (a) divergence of M_w and of τ_0 is expected at the gel point; (b) power law behavior should be found for $G'(\omega)$, $G''(\omega)$ or $G(t)$ in mechanical relaxation, and for the time correlation function $g_1(t)$ in dynamic LS experiments.

3. Experimental Section

3.1. Sample Preparation. The exocellular polysaccharide (EPS) extracted from *R. leguminosarum bv. Phaseoli* strain 8002 was isolated and purified at the AFRC Institute of Food Research, Norwich Laboratory, Norwich, U.K., by Dr. V. J. Morris as reported previously.[1]

The results of sugar and methylation analysis and the measured data of the uronic acid content for the purified EPS are consistent with the structure shown in Figure 1. The only contaminant in the 8002 sample is due to a very small quantity (<1%) of a cyclic β (1 → 2) glucan. A water content of 11% was determined for the freeze-dried polymer by thermogravimetry.

3.2. Preparation of Gels for Light Scattering. From a study of dilute solutions of the *R. leguminosarum* EPS[3] the overlap concentration was found to be $c^* = (A_2M_w)^{-1} = 3 \times 10^{-3}$ g/cm^3. To get a gel, three different samples were prepared, i.e. with concentrations of $c = 1.5\%$ (w/v) $= 5c^*$, $c = 2.0\% = 6.7c^*$ and $c = 3.0\% = 10c^*$. The polymer was first dissolved in doubly distilled water; then the proper concentration of NaCl was added, whereupon a gel is immediately formed. The gels were then heated up to 70 °C, well above the gel melting temperature, for approximately 5 min. This procedure proved to be essential to break up macroscopic aggregates that would exist even in the molten gel near the gel setting temperature. Clear and fully transparent gels were obtained after cooling to room temperature. Before the light scattering cells were filled, the gels were heated up once again and filtered in an oven at 80 °C three times through 1.2 μm Millipore sterilized one-way filters and then directly into the LS cells.

3.3. Light Scattering. Static and dynamic light scattering measurements were carried out in the angular range from 30 to 150° in steps of 10° at different temperatures (starting from 10 °C up to 55 °C). The red line ($\lambda_o = 647.1$ nm) of a Kr ion laser (Spectra Physics, Model Kr 2020) was used. Measurements were made with an ALV photogoniometer system equipped with a ALV-3000 correlator-structurator (ALV, Langen, Germany). Details of the instrument and the set up are given in ref 20.

All dynamic experiments were performed in the "multi τ" mode which allowed a logarithmic expansion of the time scale over 7 decades. At least three runs were recorded for each angle (a single run took at minimum 60 min). This procedure, together with the multi τ mode, allowed the recording of the correlation function down to the baseline.

Concerning the static measurements, the cell was rotated at least 15 times for each angle; after each turn the data were collected, and the average over the various runs was then taken.

3.4. Refractive Index Increment. The refractive index increment of the polysaccharide was measured with a Brice-Phoenix 60 differential refractometer at $\lambda_o = 647.1$ nm at 25 °C and a value of $dn/dc = 0.117 + 0.02$ cm^3/g was obtained.

4. Results

4.1. Static Scattering. 4.1.1. Light scattering. Measurements were made with the three concentrations of the polysaccharide of 1.5%, 2%, and 3% (w/v) in a 0.1 M NaCl solution in a temperature interval between 10 and 55 °C. Above a certain temperature (around 41−45 °C, depending on the concentration) typical solution behavior was observed and the measurements were not affected by difficulties.[8]

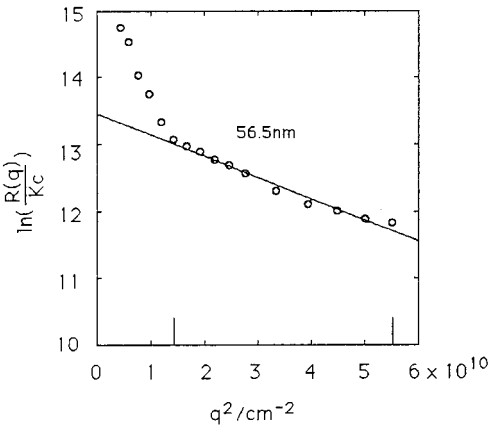

Figure 2. Guinier plot of the statc light scattering intensities of the polysaccharide *Rhiz. legum. phas.* 8002 EPS, of a 2% (w/v) gel.

At low temperatures a clear gel was obtained. In spite of the good transparency, serious problems occurred with these gels. Strong fluctuations in the scattering intensities were obtained when the cylindrical cell was rotated step by step. These fluctuations are the result of spatial inhomogeneities which are not averaged out in the short time interval (10 s) of the static LS measurements as a result of the low translational mobility of the material. Therefore, we changed the position of the scattering volume by rotating the cell around the cylindrical axis in at least 15 steps and took then for each angle the average over these measurements. We are aware that this number of repetition is not sufficiently large to get a good statistical average but there was no significant difference, within experimental error, between the scattering curves at 50 °C (solution) and those at 16 °C (gel). At the time of our measurements, no mechanical equipment was available that would perform the spatial averaging more efficiently. In the following we took for each of the three concentrations the average over all temperatures.

The result is shown in Figure 2 in which the data of Kc/R_θ were plotted logarithmically against q^2 (Guinier plot). Apparently there are two components which differ by a factor 10 in the ordinate intercept and about a factor 3.3 in the slope (Table 1). At least the initial part (30−50°, i.e. $q^2 = (0.45-1.2) \times 10^{-10}$ cm^{-2}) could be well represented by a straight line, but also the section from 60 to 110° ($q^2 = (1.7-4.5) \times 10^{-10}$ cm^{-2}) may be approximated in this manner (however, see the Discussion).

4.1.2. Small Angle X-ray Scattering. To obtain more details on the structure of the gel, small angle X-ray scattering (SAXS) measurements were carried out using the D24 instrument at LURE, Orsay, France. The measurements were made at room temperature (20 °C) with an incident wavelength of 1.49 Å, the sample-detector distance being 192 cm. Spectra were accumulated for 30 min. The absolute intensity was found by calibrating with a solution of poly(vinyl acetate) in toluene, the osmotic pressure of which is known,[21] and then multiplying by the ratio of the contrast factors. The principle error in this estimate comes from uncertainty in the value of density of the dry polysaccharide; this was taken to be 1.7 g/cm^3, which is slightly lower than

Table 1. Values for the Constants A and B, ξ, and R_G in Eq 9c, and of the Correlation Lengths ξ_1 and ξ_2, and the Chain Cross Sectional Radius r_c from Eq 10 and Figure 4[a]

	c (w/v) 1.5%	c (w/v) 2.0%	c (w/v) 3.0%
	Guinier Fit to Eq 9		
$A \times 10^{-7}$, g/mol	1.40 ± 0.10	0.95 ± 0.18	$0-91 \pm 0.12$
R_G, nm	308 ± 10	303 ± 10	308 ± 7
$B \times 10^{-5}$, g/mol	6.4 ± 0.1	6.8 ± 0.2	$3.9 \pm .0.2$
ξ, nm	54.9 ± 1	56.4 ± 1	57.6 ± 2
	Fit to eq 10		
$a_0 \times 10^{-7}$ g/mol		0.8	
R_G, nm		310	
$a_1 \times 10^{-5}$, g/mol		5.45	
ξ_1, nm		120	
$a_2 \times 10^{-3}$, g/mol		2.73	
ξ_2, nm		2.1	
r_c, nm		0.7	

[a] The values in the last five lines correspond to averages between LS and SAXS data.

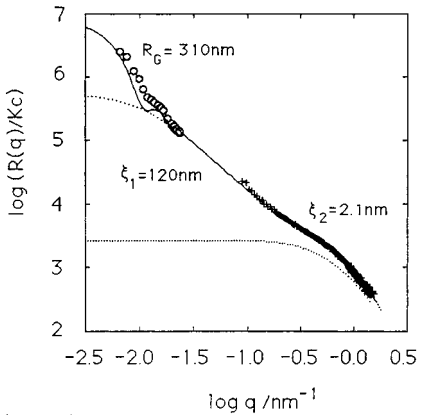

Figure 3. Total scattering spectrum of the 2% gel (+) SAXS measurements, (○) LS measurements. The components of $I_1(q)$ and $I_2(q)$ of eq 10 are shown as dotted lines, the continuous line being the total fit.

that found for a more highly carboxylated polysaccharide, a citrus pectin.[22]

4.1.3. Discussion of the Static Behavior. The static light scattering spectra suggest the presence of two characteristic length scales, in which particles with a large radius of gyration R_G coexist with smaller structures of length scale ξ. To quantify this behavior, the static light scattering data are plotted in Figure 2 on the assumption that they obey Guinier type relations in two different linear regions.

$$\left(\frac{R_\theta}{Kc}\right)_1 = A \exp\left(-\frac{R_G^2 q^2}{3}\right) \quad \text{for } q^2 < 1.2 \times 10^{10}\,\text{cm}^{-2} \tag{9a}$$

and

$$\left(\frac{R_\theta}{Kc}\right)_2 = B \exp(-\xi^2 q^2) \quad \text{for } q^2 > 1.7 \times 10^{-10}\,\text{cm}^{-2} \tag{9b}$$

such that the whole angular dependence of the LS is given by the sum of two corresponding intensities

$$\left(\frac{R_\theta}{Kc}\right) = \left[A \exp\left(-\frac{R_G^2 q^2}{3}\right) + B \exp(-\xi^2 q^2)\right] \tag{9c}$$

The prefactors and characteristic lengths, determined by a nonlinear least square fit to eq 9c, are listed in Table 1. It should be recalled, however, that the numerical value of the second characteristic length, ξ, as it is obtained from a region of the spectrum in which $q\xi > 1$, depends heavily on the form chosen for the fitting function. For example, replacing the Guinier representation by a Zimm plot for this region yields a value for ξ more than twice as large as that quoted in Table 1.

The presence of two different length scales in Figure 2 and the suggestion of a damped oscillation that is visible in the response indicate that eq 9c does not yield a complete description of the system. Extra information on the structure is to be found in the small angle X-ray scattering spectrum. This is shown in Figure 3, in a double logarithmic scale, together with the LS data from the same 2% sample and expressed in the same absolute units. Although there is a gap in the q-range between the two sets of data, there is no reason to suppose that the spectrum in the gap is not continuous.

In the double logarithmic representation in Figure 3, three principal regions can be distinguished. At the lowest q value in the light scattering region a damped oscillatory component is noticeable, followed at intermediate q by a linear region of approximate slope -1.6. At still higher q a shoulder appears in the spectrum near $q = 0.5$ nm^{-1} (log $q = -0.3$), beyond which the intensity drops sharply. As no scattering function with a single characteristic length is capable of describing the complete spectrum, each feature must be considered separately.

First the oscillatory behavior observed at low q is characteristic of dense particles having a fairly well-defined size. Owing to its mathematical convenience, one of the easiest particle scattering function to handle is that of the sphere.[23] Other regular shapes, however, such as the cube and the parallelepiped,[24] generate similar oscillatory spectra whose important characteristic is that the initial minima coincide with those of a sphere having the same radius of gyration R_G. For these and other shapes the minima are attenuated compared to those of a sphere. Even though the system of particles is almost certainly polydisperse, for our present purpose it is sufficient to use the single particle scattering function of a sphere

$$I_0(q) = a_o\left(\frac{\sin x - x \cos x}{x^3}\right)^2 \tag{10a}$$

where $x = (3/5)^{1/2} q R_G$, and a_o is a constant.

Comparison of the position of the minima gave for the best fit to this component a radius of gyration $R_G = 310$ nm, in acceptable agreement with that found above from the Guinier fit. Although the concentration of particles giving rise to this scattering is unknown, it is certainly small since the gels are highly transparent. The use of a single particle scattering factor is therefore justified here. The mass of the particles, however, remains undetermined since their concentration is unknown.

Second, the intermediate q behavior and the shoulder around $q \approx 0.5$ nm^{-1} are features that are familiar in neutral gels,[25-27] In these systems the scattering in the intermediate q range is due to large scale inhomogeneities resulting from the balance between osmotic forces and topological constraints of the cross-links and entanglements; the shoulder comes from dynamic concentration fluctuations associated with the overall osmotic response of the gel. The two corresponding lengths are denoted by ξ_1 and ξ_2 , respectively, of which ξ_1 now takes the part of the second length in eq 9c.

In the past, several fitting formulas have been proposed for these components ξ_1 and ξ_2 in gel spec-

tra.[25,26,29,42,43] In the present case, the intermediate region with a slope close to −1.6 in the double logarithmic plot argues in favor of a model proposed by Bastide et al.[26] This model interprets the swelling of a gel as a disinterpenetration of branched clusters. Their suggested expression for the scattering function is

$$I_1(q) = \frac{a_1}{[1 + g(q)q^2\xi_1^2]} \tag{10b}$$

where

$$g(q) = \frac{1}{1 + (q\xi_1)^{2-d_f}} \tag{10c}$$

The fractal dimension $d_f = {}^8/_5$ corresponds to the cluster size distribution discussed in ref 26. Expression 10b is not, however, compatible with the observed spectrum because it fails to vanish fast enough at high q. This difficulty can be overcome by applying a cut-off factor $[1 + g(q)qr_c/\sqrt{2}]\exp(-q^2r_c^2/2)$ to eq 10b that accounts for the finite radius r_c of the polymer strands such that

$$I_1(q) = \frac{a_1}{[1 + g(q)q^2\xi_1^2]}[1 + g(q)qr_c/\sqrt{2}]\exp(-q^2r_c^2/2) \tag{10d}$$

The optimum value for r_c in the present fit was found to 0.7 nm.

The last component in the scattering spectra of soft gels is that of thermally excited concentration fluctuations. This component, not treated explicitly in ref 26, is nonetheless essential since it is associated with the osmotic pressure. The corresponding correlation length ξ_2 has the same role as in semidilute polymer solutions. In photon correlation spectroscopy it gives rise to the osmotic breathing, or gel mode.[27] It can be represented here by a modified Ornstein−Zernike form[28,29]

$$I_2(q) = \frac{a_2}{1 + q^2\xi_2^2}\left(1 + \frac{qr_c}{\sqrt{2}}\right)\exp\left(-\frac{q^2r_c^2}{2}\right) \tag{10e}$$

The cut-off factor is similar to that for $I_1(q)$, and the constant a_2 is given by

$$a_2 = \frac{kTc^2}{M_{OS}}$$

where M_{OS} is the longitudinal osmotic modulus of the gel.[27,29] In the present case independent measurements of the osmotic pressure of the gels were not available: both a_1 and a_2 are therefore treated as adjustable parameters in the fitting procedure.

The total scattering function is then represented by the sum $I_0(q) + I_1(q) + I_2(q)$. In Figure 3 the components $I_1(q)$ and $I_2(q)$ of the scattering function appear as dotted lines, the total scattering function being the continuous curve. We recall again that the fit to the low q region exaggerates the amplitude of the oscillations in the experimental curve: its use here merely shows the coincidence of the positions of the minima. The parameters for this fit are listed in Table 1.

The threefold heterogeneity observed with this bacterial polysaccharide is not the first example of such behavior. Horkay et al.[30] found a two-step behavior, and recently Kajiwara et al.[31] observed a similar three-step scattering curve for methylhydroxypropyl cellulose gels in water.

In the present case further information about the large compact objects can be deduced from their scattering intensity. The dense packing of their chains, indicated by their scattering behavior, is best achieved by side-by-side alignment as is the case for fringed micelles in the molten state. The value of a_0 corresponding to R_Θ/Kc, listed in Table 1, is based on the assumption that the concentration is $c = 0.02$ g/cm^3, i.e. the overall concentration in the sample. Although the true concentration of these associates is unknown, it can be estimated on the assumption that the particles are approximately isotropic (e.g. cubes or polydisperse spheres). Their mass M is then equal to $(4\pi/3)\rho R_G^3$, where ρ is the density of the dry polymer, and their number density is n. Their concentration thus becomes $c = n[(4\pi/3)\rho R_G^3]$, and we therefore can set

$$cM = nN_A[(4\pi/3)\rho R_G^3] = R_\Theta/K \tag{11}$$

where N_A is Avogadro's number. This yields for the number density

$$n \approx 10^7 \text{ cm}^{-3}$$

It is reasonable to expect that these folded objects, connected to the network by the polymer strands, act as cross-links. If these were the only cross-links present they would give rise to an elastic shear modulus $G = nkT$. For the present gels G lies in the range 100−1000 Pa. corresponding to $n \approx 10^{16}$−10^{17} cm^{-3}. This cross-link density is thus many orders of magnitude larger than the large particle density estimated from the light scattering intensity. We therefore conclude that the particles are extremely sparse and make no significant contribution to the elasticity of the system. This conclusion also confirms the justification for our neglect of inter-particle scattering at small angles in eq 10a. However, these dense particles are probably only the cores of fringed micellar structures with many outgoing chains which via association will produce the gel.

The above explanation for the large particles simplifies the interpretation of the hierarchy of other lengths in the system. According to the model by Bastide et al.[26] the cross-link distribution is very broad, the upper bound being by $\xi_1 = 120$ nm. This is sketched in Figure 4 as the distance between one densely cross-linked region and another. Although the average spacing between cross-links R_x is not measured it can be deduced from the above estimate of the shear modulus, $G = nkT = 3kT/(4\pi R_x^3)$, which yields $R_x \approx 10$ nm. Finally, the thermal fluctuations whose correlation length is $\xi_2 = 2.1$ nm and which is shown in Figure 4 as a nearest distance of approach between chains giving rise to intensity fluctuations in a dynamic light scattering experiment. Because of the fairly long side chain this distance is somewhat larger than the chain diameter. The relaxation time for the corresponding field correlation function is, from eq 2

$$\tau = \frac{6\pi\eta\xi_2 f_H}{kTq^2} \tag{12}$$

where η is the solvent viscosity. The factor f_H is the ratio of the hydrodynamic to the static correlation length which according to scaling arguments is $f_H \approx 1.5$.[32,33] For example, a measurement with light of the wave-

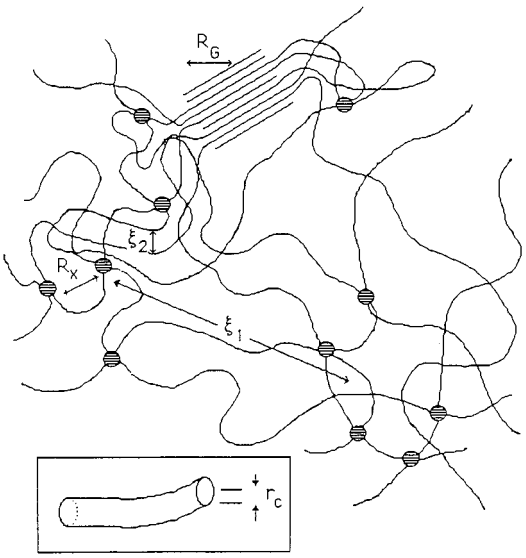

Figure 4. Schematic diagram of the length scales prevailing in the gel. R_G is the radius of gyration of the sparse precipitate structures. ξ_1 is the separation between regions of higher (or lower) cross-linking density, and ξ_2 is the correlation length describing the spectrum between chains. The cross-links are represented by shaded circles, their mean separation being R_x. The inset represents a short chain segment of radius r_c, In this sketch, the difference in polymer concentration between dense and more dilute regions is greatly exaggerated.

length 647.1 nm yields with $\xi_2 = 2.1$ nm a decay time of approximately 5×10^{-5} s.

As for the cross-sectional radius of the polymer chain, r_c, the value found from the SAXS spectra is at 0.7 ± 0.1 nm in reasonable agreement with that found previously in solution,[3] namely 0.78 nm.

4.2. Dynamic Light Scattering. 4.2.1. Experimental Results. The dynamic light scattering measurements were made with the same samples, i.e. the same concentrations and the same temperatures as for static LS. Because of the wide spread of relaxation times measurements were made in the "multi τ" mode of the autocorrelator, i.e. the delay time t is spaced pseudologarithmically (16 equally spaced delay times for the first 16 channels, after that the spacing time is doubled again, etc.). A total of 192 channels were used which allowed delay times from 10^{-6} s up to 10^3 s. To achieve a good accuracy, a 1 h recording at least was needed. The measurements were repeated at least three times or more. A much weaker fluctuation of the data were found after such a long time than observed in static LS, where recording times of only 10 s to about 30 s were applied. Evidently a recording time of 1 h was already sufficiently long to guarantee a satisfactory time averaging that equals the ensemble average.

The evaluation of the scattering intensity time correlation function (TCF), $G_2(t) = \langle i(0)i(t)\rangle$ turned out to be not correlated to the field TCF via the Siegert relationship since significant heterodyne contribution became noticeable when passing the gel point. Thus instead of the Siegert relationship one has to use a more general approach based on the partially heterodyne dynamic LS which is given by[34]

$$g_2(t) = 1 + \beta[2X(1 - X)g_1(t) + X^2 g_1^2(t)] \quad (13)$$

where

$$g_2(t) = \langle i(0)i(t)\rangle / \langle i(0)^2\rangle$$

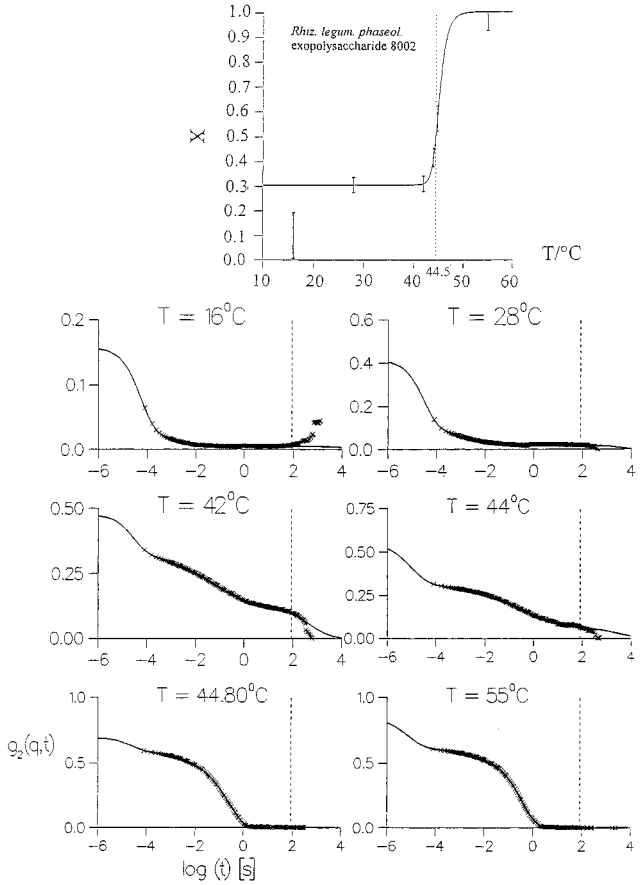

Figure 5. Intensity time correlation functions $g_2(t) - 1$ at $\theta = 90°$ for some selected temperatures $c = 2\%$(w/v). Inset: Homodyne contribution X as function of T (°C). The inversion point can be taken as the gel point, which agrees well with the qualitative test tube tilting test.

The parameter X can lie between zero and unity; X^2 denotes the homodyne and $2X(1 - X)$ represents the heterodyne contribution. $X = 1$ describes full homodyne contribution while at lower values the heterodyne contribution eventually becomes dominant. Figure 5 shows an example of $[g_2(t) - 1]$ at 90° for different temperatures. One notices a drastic decrease of the correlation strength at the lowest delay time that was applied when cooling the system below the gel setting temperature. This decrease is an effect of the heterodyne scattering. The intercept at delay time $t \rightarrow 0$ is $\beta[2X - X^2]$ from which the value of X can be estimated if β is known. This $\beta \leq 1$ value is an instrumental factor and can be determined from an experiment at high temperatures where the molten system shows no heterodyne effects. The change of the homodyne contribution with temperature is shown in the insert of Figure 5.

In order to get more reliable results from these intercepts a nonlinear Laplace inversion of eq 13 was made where $g_1(t)$ is given by eq 8. Such an inversion program was recently developed by Honerkamp et al.[35] which resulted in relaxation spectra of Figure 6 at different temperatures. Other examples which cover the angular dependence are described below. The vertical dashed lines indicate the area of reliable relaxation times while the full lines where obtained after applying a regularization method as described in the Appendix. The same procedure has been performed for two temperatures (corresponding to gel and solution states) as a function of scattering angle which are given in Figure 7.

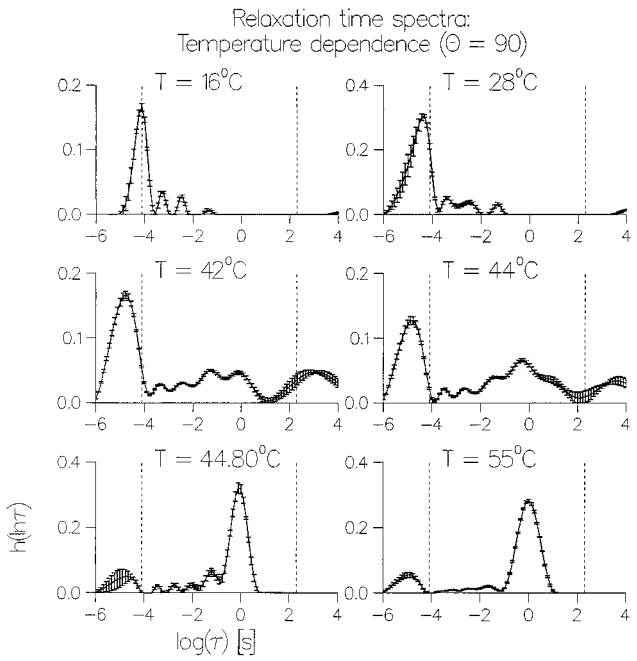

Figure 6. Relaxation time spectra at different temperatures ($\theta = 90°$) for $c = 2\%$(w/v).

4.2.2. Discussion of the Dynamic LS Data. First the *correlation strength* at zero time may be discussed. The insert of Figure 5 shows the temperature dependence of the homodyne fraction X defined in eq 13. This value exhibits a sharp decrease down to $X = 0.3$ on passing the gel point. An inversion point is obtained at 44.5 °C, which may be taken as the gel point. The spectrum obtained with the regularization technique of Honerkamp et al.[35] shows a somewhat unexpected structure. At 55 °C (solution) two dominant peaks are visible. The slow component is probably associated with the translational diffusion of large particles while the faster one can be assigned to the gel mode that governs the exchange of solvent and polymer in the temporary network. When the gel point is passed, the slow motion becomes less dominant and eventually disappears completely, as expected for the translational diffusion of large objects in a gel. The fast motion increases in importance and moves now into the region of reliability, indicating that this motion as being not an artefact even for the higher temperatures. These two peaks, slow and fast, are in agreement with the results of static LS which revealed a heterogeneous structure: The decay time of the fast mode, as expected from the value of the correlation length ξ_2, is indeed approximately 5×10^{-5} s. This result confirms the earlier assignment of ξ_2 as the correlation length of the thermal fluctuations. However, the many smaller peaks in the intermediate time region are unexpected. Instead of the observed discrete relaxations a continuous power spectrum of relaxation times was expected that obeyed a power law at the gel point. It seems probably that the many discrete peaks are an artefact of the regularization procedure and the inverse Laplace transformation, in spite of the improved technique of nonlinear regularization. A better resolution of the spectrum might be possible with the much improved ALV 5000 correlator, but we rather think that all available inversion programs are intrinsically incapable of properly describing a power law behavior in term of a continuous relaxation distribuition.

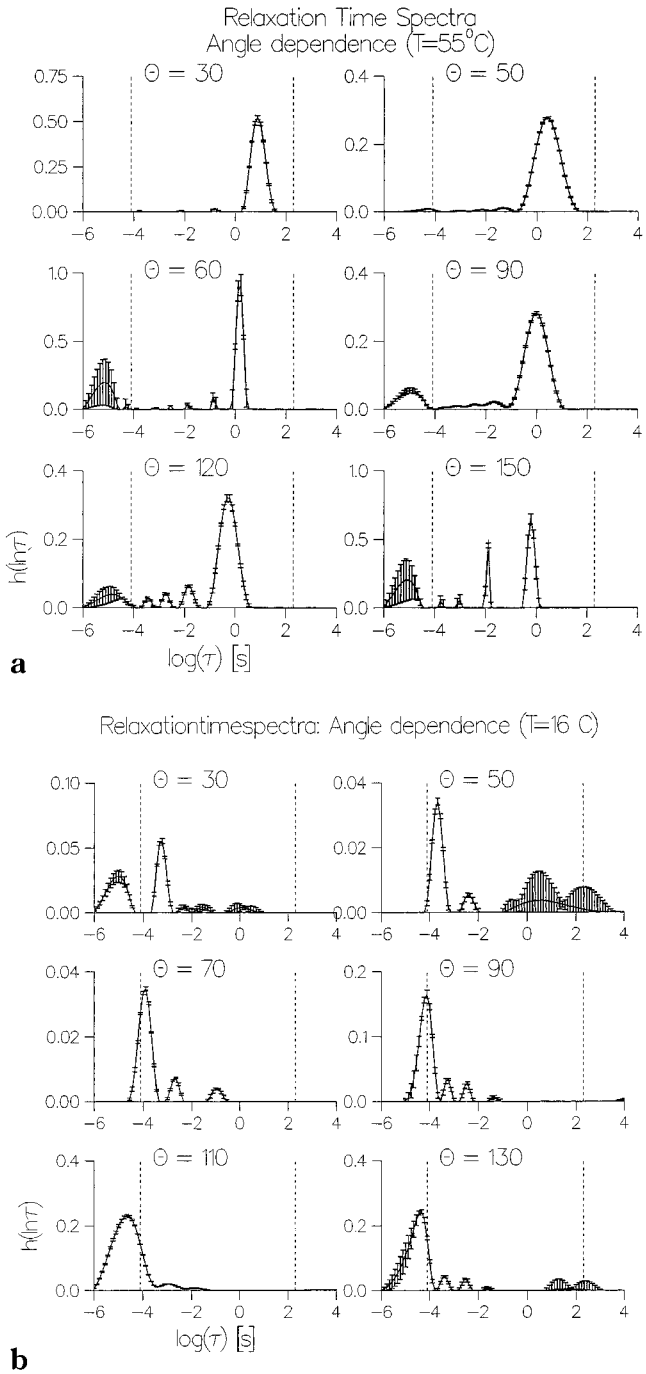

Figure 7. Relaxation time spectra as a function of the scattering angle: (a) $T = 55$ °C; (b) $T = 16$ °C.

Acknowledgment. T.C. thanks the NATO-CNR "Advanced Fellowship Program" foundation for a postdoctoral stipend. W.B. thanks the Deutsche Forschungsgemeinschaft for financial support within the SFB 60 scheme. We are also grateful for access to the D24 beam line of the DCI synchrotron at LURE, Orsay, France.

Appendix

Nonlinear Laplace Inversion. The problem is to find a good estimation of the relaxation spectrum $h(\ln \tau)$ for a given set of noisy TCF data $g_2^{\tau}(q,t_i)$, $i = 1, 2, ..., n$, which is an *ill-posed problem*, and special techniques have to be employed to solve this problem. (for definition of an *ill-posed problem* see ref 36). One of the techniques consists of the Tikhonov regularization which requires the minimization of a function $V(\lambda)$ that

is given as[37,38]

$$V(\lambda) = \left\{ \frac{g_2{}^{\sigma}(t_i) - [\sum_{-\infty}^{+\infty} h(\ln \tau) e^{-t/\tau} \, d(\ln \tau)]^2}{\sigma^2} \right\}^2 + \lambda ||h||^2 \tag{A1}$$

In this relationship $g_2{}^{\sigma}(t_i)$ denotes the measured quantities at delay time t_i, ($i = 1, 2, ..., n$), and n is the number of channels which are imposed by the corresponding errors σ_i. These errors can be estimated in a relationship that was derived by Schätzel.[39] The σ_i values depend on the delay times τ_i on the values of the electric field TCF $g_1(t_i)$ which are related to $g_2(t_i)$, and on β via eq 13. Most important is the last term $\lambda||h||^2$, which produces the regularization where $||h||^2$ is the norm of the relaxation spectrum that is given by

$$||h||^2 = \sum_{-\infty}^{+\infty} h^2(\ln \tau) \, d(\ln \tau) \tag{A2}$$

The necessity of regularization requires some words of explanation. In cases where the general type of the spectrum is known in the form of a well-defined function which only depends on some unknown parameters the last term in eq A1 is zero. The result is that in this case one has to estimate only a finite set of parameters, and therefore, a conventional least-square fit is sufficient. However, in the present case of a TCF the spectrum is not known, and therefore, a complete function must be fitted. Since any function is represented by an infinite set of parameters one must use a nonparameter method. The regularization method is such a nonparameter method and is needed for this application.

The problem which here arises is to find a good value for λ. With a given λ the quantity V(λ) is minimized with respect to h (see eq A1). A naive method to get a good value for the regularization parameter is the visual method where λ is varied; then that relaxation spectrum is chosen that is considered to be the best. In the present treatment the procedure starts with an arbitrary λ. Then a best value for λ is obtained by a self-consistent method that was derived by Weese et al.[40,41] Here one has to search the minimum of the expectation value

$$E(\lambda,h) = \langle d(\lambda,h) \rangle \tag{A3}$$

with respect to λ where

$$\langle d(\lambda,h) \rangle = ||h^{\lambda} - h|| \tag{A4}$$

With the new value of λ the process starts again. The regularizatíon term causes a smoothing of the spectrum which is essential since otherwise the minimization would result in an uncontrolled fluctuation of the spectrum. Furthermore, for physical reasons the spectrum must not become negative at any point, and all these solutions which are mathematically possible have to be discarded.

References and Notes

(1) Morris, V. J.; Brownsey, G. J.; Harris, J. E.; Gunning, A. P.; Stevens, B. J. H.; Johnston A. W. B. *Carbohydr. Res.* **1989**, *191*, 315.

(2) (a) Dentini, M.; Coviello, T.; Burchard, W.; Crescenzi, V. *Macromolecules* **1988**, *21*, 3312. (b) Coviello T., Crescenzi, V.; Dentini, M. .Cesaro, A. *Polymer* **1990**, *31*, 834.

(3) Coviello, T.; Burchard, W.; Dentini, M.; Crescenzi, V.; Morris, V. J. *J. Polym. Sci., Part B: Polym. Phys.* **1995**, *33*, 1833.

(4) Clark, A. H.; Ross-Murphy, S. B. *Adv. Polym. Sci.* **1987**, *83*, 57.

(5) Lehninger, A. L. *Biochemistry*; Worth Publishers: New York, 1979.

(6) (a) Sandford,P. A. *Adv. Carbohydr. Chem. Biochem.* **1979**, *36* Academic Press. (b) Sharon, N. *Complex Carbohydrates: Their Chemistry, Biosynthesis and Functions*, Addison-Wesley Publishing Company-Advanud Book Program: Reading, MA, 1975.

(7) (a) *Advances in Nitrogen Fixation Research, Proceedings of the International Symposium on Nitrogen Fixation, 5th*; Edited by Veeger, C., Newton, W. E. N., Eds.; Niihoff: Dordrecht, The Netherlands, 1984. (b) Casas, I. A. In *Biological Nitrogen Fixation, Ecology, Technology and Physiology*; Alexander, M., Ed.; Plenum Press: New York, 1984; pp 99−125.

(8) Crescenzi, V.; Dentini, M.; Coviello, T. In *New Developments in Industrial Polysaccharides*; Crescenzi, V., Dea, I. C. M., Stivala, S. S., Eds.; Gordon & Breach: New York 1987; pp 69−97.

(9) Stauffer, D. *Introduction to Percolation Theory*; Taylor & Francis: Philadelphia, PA, 1985.

(10) Almdal, K.; Dyre, J.; Hvidt, S.; Kramer, O. *Polym. Gels Networks* **1993**, *1*, 5.

(11) (a) Winter, H. H.; Chambon, F. *J. Rheol.* **1986**, *30*, 367. (b) Winter, H. H. *Polym. Eng. Sci.* **1987**, *27*, 1698.

(12) Burchard, W.; Lang, P.; Schulz, L.; Coviello, T. *Makromol. Chem., Macromol. Symp.* **1992**, *58*, 21.

(13) Auersch, A.; Littke, W.; Lang, P.; Burchard, W. *J. Cryst. Growth* **1991**, *110*, 201.

(14) Schulz, L.; Burchard, W. *Papier* **1989**, *43*, 665.

(15) Schosseler, F.; Benoit, H.; Grubisic-Gallot, Z.; Strazielle, C.; Leibler, L. *Macromolecules* **1089**, *22*, 400.

(16) Patton, E. V.; Wesson, J. A.; Rubinstein, M.; Wilson, J. C.; Oppenheimer, L. E. *Macromolecules* **1989**, *22*, 1946.

(17) Bauer, J.; Lang, P.; Burchard, W.; Bauer, M.; *Macromolecules* **1991**, *24*, 2634.

(18) Daoud, M.; Martin, J. E. In *The Fractal Approach to Heterogeneous Chemistry*; Avnir, D., Ed.; John Wiley & Sons: New York, 1989; pp 109−130.

(19) Martin, J. E. *Macromolecules* **1986**, *19*, 1278.

(20) Bantle, S.; Schmidt, M.; Burchard, W. *Macromolecules* **1982**, *15*, 1604.

(21) Vink, P. *Eur. Polym. J.* **1974**, *10*, 149.

(22) Harding, S. *Carbohydr. Polym.* **1991**, *16*, 1.

(23) Rayleigh, Lord *Proc. R. Soc. London* **1911**, *A-84*, 25.

(24) Porod, G. *Kolloid-Z.* **1951**, *124*, 83.

(25) Mallam, S.; Hecht, A. M.; Geissler, E.; Pruvost, P. *J. Chem. Phys.* **1989**, *91*, 6447.

(26) Bastide, J.; Leibler, L.; Prost, J. *Macromolecules* **1990**, *23*, 1821.

(27) Tanaka, T.; Hocker, L. O.; Benedek, G. B. *J. Chem. Phys.* **1973**, *59*, 5151.

(28) Ornstein, L. S.; Zernicke, E. *Proc. Acad. Sci.—Amsterdam* **1914**, *17*, 793.

(29) Horkay F.; Hecht A. M.; Mallam, S.; Geissler, E.; Rennie, A. R. *Macromolecules* **1991**, *24*, 2896.

(30) Horkay, F.; Burchard, W.; Hecht, A. M.; Geissler, E. *Macromolecules* **1993**, *26*, 3375.

(31) Yugushi, Y.; Urakawa, H.; Kitamura. S.; Ohono, S.; Kajiwara, K. *Food Hydrocolloids* **1995**, *9*, 173.

(32) Daoud, M.; Cotton, J. P. Farnoux, B.; Jannink, G.; Sarma, G.; Benoit, H.; Duplesix, R.; Picot, C.; de Gennes, P.-G. *Macromolecules* **1975**, *8*, 804.

(33) Adam, M.; Delsanti, M. *Macromolecules* **1977**, *10*, 1229.

(34) Geissler, E. In *Dynamic Light Scattering*; Brown, W., Ed.; Clarendon Press: Oxford, England, 1993.

(35) Honerkamp, J.; Maier, D., Weese, J. J. *J. Chem. Phys.* **1993**, *98*, 2.

(36) Morovoz, V. A. *Methods for Solving Incorrectly Posed Problems*; Springer: Berlin, 1984.

(37) Groetsch, C. W. *The theory of Tikhonov Regularization for Fredholm Equations of the First Kind*; Pitman: London, 1984.

(38) Vogel, G. R.; Siam, J. *Control Optimization* **1990**, *28*, 34.

(39) Schätzel, K. *Quantum Opt.* **1990**, *2*, 287.

(40) Honerkamp, J.; Weese, J. *Continuum Mech. Thermodyn.* **1990**, *2*, 17.

(41) Weese J., *Comput. Phys. Commun.* **1993**, ***77***, 429.

(42) Falcao, A,N.; Pedersen, J. S.; Mortensen, K. *Macromolecules* **1993**, *26*, 5350.

(43) Falcao, A. N.; Pedersen, J. S.; Mortensen, K.; Boué, F. *Macromolecules* **1996**, *29*, 809.

MA961651B